

UNCLASSIFIED

Defense Technical Information Center
Compilation Part Notice

ADP012531

TITLE: Experimental Observation of Fluid Echoes in a Non-Neutral Plasma

DISTRIBUTION: Approved for public release, distribution unlimited

This paper is part of the following report:

TITLE: Non-Neutral Plasma Physics 4. Workshop on Non-Neutral Plasmas [2001] Held in San Diego, California on 30 July-2 August 2001

To order the complete compilation report, use: ADA404831

The component part is provided here to allow users access to individually authored sections of proceedings, annals, symposia, etc. However, the component should be considered within the context of the overall compilation report and not as a stand-alone technical report.

The following component part numbers comprise the compilation report:

ADP012489 thru ADP012577

UNCLASSIFIED

Experimental Observation of Fluid Echoes in a Non-Neutral Plasma

Jonathan H. Yu and C. Fred Driscoll

*Dept. of Physics and Institute for Pure and Applied Physical Sciences,
University of California at San Diego, La Jolla CA 92093-0319 USA*

Abstract. Experimental observation of a nonlinear fluid echo is presented which demonstrates the reversible nature of spatial Landau damping, and that non-neutral plasmas behave as nearly ideal 2D fluids. These experiments are performed on UCSD's CamV Penning-Malmberg trap with magnetized electron plasmas. An initial $m_i = 2$ diocotron wave is excited, and the received wall signal damps away in about 5 wave periods. The density perturbation filaments are observed to wrap up as the wave is spatially Landau damped. An $m_i = 4$ "tickler" wave is then excited, and this wave also Landau damps. The echo consists of a spontaneous appearance of a third $m_e = 2$ wave after the responses to the first two waves have inviscidly damped away. The appearance time of the echo agrees with theory, and data suggests the echo is destroyed at least partly due to saturation.

Longitudinal plasma wave echoes have been previously observed in a neutral plasma [1], and here we present observation of diocotron wave echoes in a pure electron plasma. Diocotron waves vary as $\delta n(r, \theta) = \tilde{\delta} n(r) \exp[i(m\theta - \omega t)]$, with essentially no z -variation. These waves can be considered low frequency $\mathbf{E} \times \mathbf{B}$ drift modes representing surface waves or bulk shape distortions of the electron column. The diocotron mode damping seen here is a result of spatial Landau damping [2]. The echo's existence depends on the reversibility of the phase mixing process, and thus demonstrates the reversible nature of spatial Landau damping.

Theory predicts that echoes occur in ideal (incompressible and inviscid) 2D fluids [3], and the echo has been studied numerically in 2D fluid shear flows [4]. In the 2D $\mathbf{E} \times \mathbf{B}$ drift approximation, the dynamics of electrons in a pure electron plasma are isomorphic to that of an ideal 2D fluid. The density, drift velocity, and electrostatic potential of the electron plasma correspond to the vorticity, velocity, and streamfunction of the 2D ideal fluid, respectively [5]. Detecting the echo in a non-neutral plasma is striking, since one might think that non-ideal effects would destroy phase information in the density distribution.

The diocotron waves and echoes are excited and received using wall sectors of a cylindrical Penning-Malmberg trap. Fig. 1 is an oscilloscope trace of the signal received from opposite 60° wall sectors. This detection scheme gives a maximum response to $m = 2$ perturbations.

An initial $m_i = 2$ wave is excited by applying $V_i = 5 - 30V$ to two opposite 60° wall sectors (different from the detection sectors) for about one half of an $m = 2$ period. The first pulse of Fig. 1 is the signal received as the initial wave of amplitude A_i decays in about five oscillations due to spatial Landau damping. A second $m_i = 4$ "tickler" wave is then excited a time τ after the initial wave is excited. The tickler wave is excited by

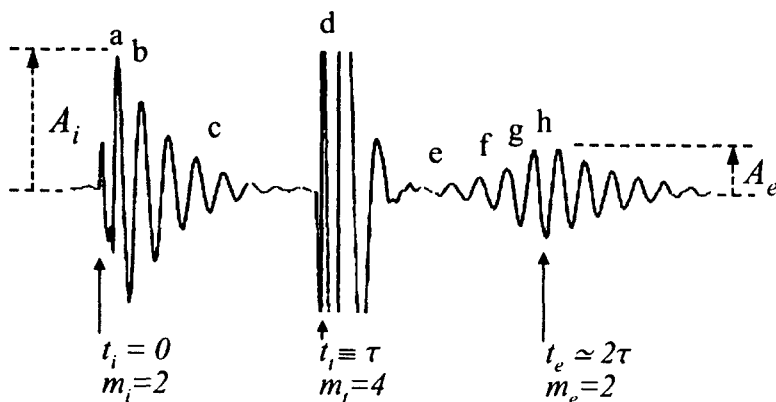


FIGURE 1. The signal received from two opposite sectors of a wall cylinder shows the initial, tickler, and echo waves.

applying a square pulse of $V_t = 1 - 40V$, for about one half of an $m_t = 4$ period, to four 30° sectors each separated by 90° . The second pulse of Fig. 1 shows the time at which the $m_t = 4$ tickler wave is excited. This signal is not actually the $m = 4$ plasma oscillation, but rather a direct coupling of the tickler excitation to the wall detector. The third wave packet of Fig. 1 is the received echo, and the peak echo response occurs at a time $t_e \approx 2\tau$. The peak echo amplitude is denoted A_e .

We have also imaged the spatial evolution of the electron density during wave damping and echo generation. At a chosen time in the evolution, the plasma is dumped onto a phosphor screen and recorded by a CCD camera. The perturbation images shown in Fig. 2 are created by subtracting a θ -symmetric density image from the density image of the perturbed plasma, giving $\delta n(r, \theta, t)$. These images directly represent phase space evolution, since angular momentum is proportional to r^2 in our magnetized electron plasma. Thus, the filamentary images illustrate the theory concepts of phase mixing (and un-mixing).

The first three images of Fig. 2 show the initial $m_i = 2$ wave forming spiral filaments as the perturbation evolves in the sheared background. The images in Fig. 2 correspond to the times labelled by the letters in Fig. 1. The $m_t = 4$ wave is excited in Fig. 2d, and the thin filaments are the remnants of the initial wave. The tickler wave nonlinearly interacts with these remnants, producing an $m_e = 2$ echo response which peaks in Fig. 2h.

Theory gives an expression for the time of the echo appearance, and this expression agrees with experiments. In the resonance layer where $\omega_E(r) = \omega/m$, the initial perturbation can be written as $\tilde{\delta}n_i(r)\exp[im_i(\theta - \omega_E(r)t)]$. Likewise, the tickler perturbation varies as $\tilde{\delta}n_t(r)\exp[im_t(\theta - \omega_E(r)(t - \tau))]$, but also modulates the initial wave. This cre-

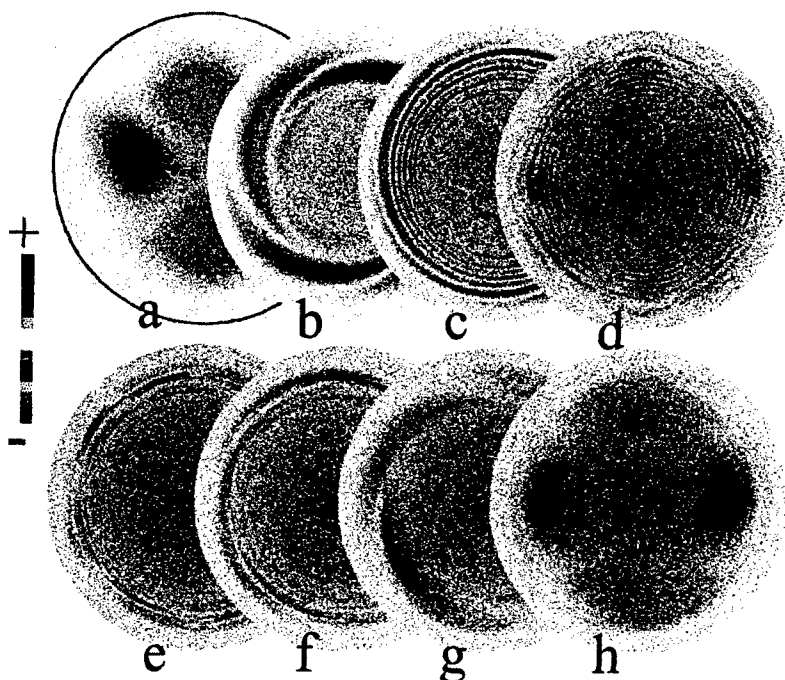


FIGURE 2. Density perturbation images at the eight successive times marked in Fig. 1. Figs. a, d, and h show the initial, tickler, and echo waves at maximal amplitude. Figs. a - c show the spiral density filamentation and wind-up of strong spatial Landau damping. Figs. f - h show the "unwinding" which creates the echo.

ates a second order perturbation varying as

$$\delta n_e(r, \theta, t) = \tilde{\delta} n_i(r) \tilde{\delta} n_t(r) \exp[i(m_t - m_i)\theta + im_t \omega_E(r)\tau - i(m_t - m_i)\omega_E(r)t]. \quad (1)$$

The time of the peak echo response occurs when a radial integral over the perturbation in Equation (1) does not phase mix to zero, and this occurs when the phase has no radial dependence [6]. Equating the ω_E terms of Equation (1) to zero yields the time of the peak echo response

$$t_e = \tau m_t / (m_t - m_i). \quad (2)$$

At this time the echo perturbation in Equation (1) has a θ dependence of $m_e = m_t - m_i$. This mode number expression agrees with the observed $m_e = 2$ structure of the echo.

We find that the predicted time for the echo response, given by Equation (2), fits the data. Fig. 3 shows the measured time of the echo response t_e , versus the time of the

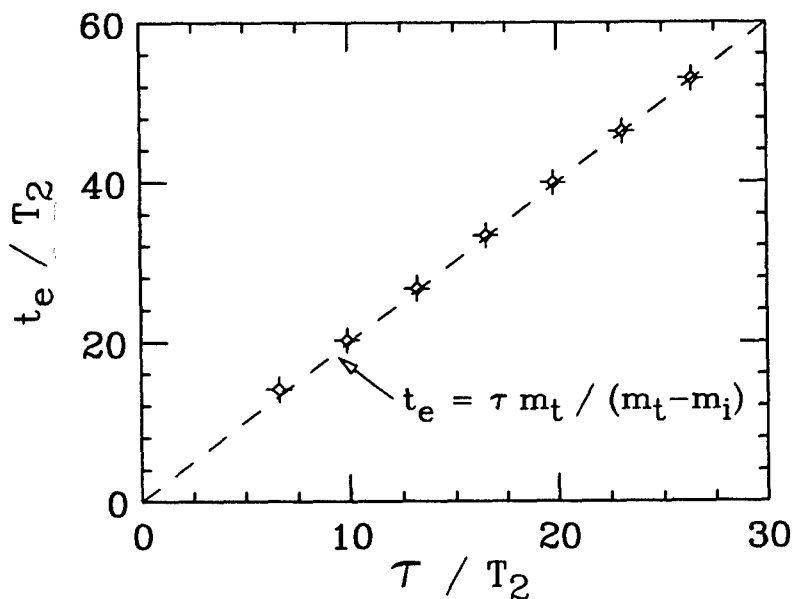


FIGURE 3. Measured time t_e of the peak echo response versus tickler delay time τ .

tickler launch τ , both scaled by $m = 2$ wave periods T_2 . The theoretical line $t_e = 2\tau$ is shown as a dashed line.

The initial and tickler waves do not have symmetric roles in their interaction leading to the echo. Fig. 4 shows the echo amplitude A_e , measured at $t = t_e$, versus τ , for four different (V_i, V_t) combinations. A_e increases approximately linearly for small τ , and then peaks and decreases at larger τ . τ_{max} is defined as the tickler launch time which results in the maximum measured echo amplitude. We find τ_{max} does not depend on A_i (see dashed curves of Fig. 4). However, the solid curves of Fig. 4 show that τ_{max} does depend on A_t . In addition, the three curves with $V_i = 15V$ give nearly the same A_e at τ_{max} .

The observed asymmetry in initial and tickler wave roles is consistent with the theory idea of saturation destroying the echo at large τ . A ballistic theory for the echo amplitude yields $A_e(t = t_e) \propto A_i J_1(\beta A_t \tau)$, where J_1 is a Bessel function of the first kind, and β is a function of m_i and m_t [6]. A_t is the maximum tickler wave amplitude and is assumed to be proportional to the applied V_t . The initial wave amplitude A_i determines the echo amplitude A_e at τ_{max} , while the tickler wave amplitude A_t determines τ_{max} itself. These theory results agree with the curves in Fig. 4, indicating that saturation is at least partly responsible for the decrease of A_e at large τ .

Theory of echo saturation yields as many as 300 $m = 2$ wave periods in τ_{max} , while experiments give no more than about 50 $m = 2$ wave periods. The discrepancy between theory and experiment at small tickler wave amplitudes suggests that non-ideal effects

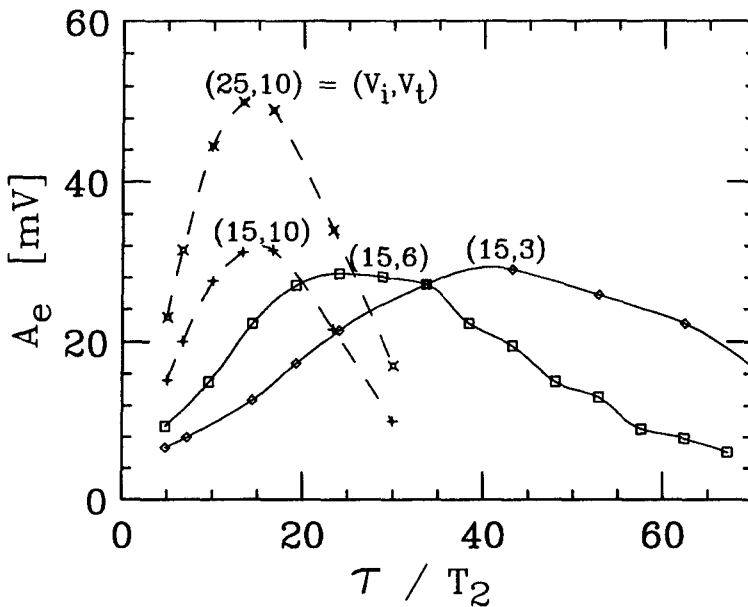


FIGURE 4. Measured amplitude A_e of the echo at $t = t_e$ versus τ . The numbers in parenthesis are the initial and tickler external excitations in volts. The decrease in echo amplitude at large τ is due at least partly to saturation.

may destroy the echo. One non-ideal effect is the magnetron drifts resulting from the end confinement fields, which cause θ -smearing [7] and which would presumably kill the echo. In addition to θ -smearing, viscosity can also wreak havoc on the ideal 2D fluid isomorphism. As the density perturbation filaments wind up, the radial spacing between filaments decreases and the filaments become thinner. After sufficient spiral wind-up the radial gradients would approach a magnitude for which viscosity is appreciable, and phase information would be destroyed. The influence of these non-ideal effects on the echo will be pursued in future work.

ACKNOWLEDGMENTS

This work was supported by Office of Naval Research grant N00014-96-1-0239 and National Science Foundation grant PHY-9876999.

REFERENCES

1. J. H. Malmberg, C. B. Wharton, R. W. Gould and T. M. O'Neil, *Phys. of Fluids* **11**, 6 (1968); D. R. Baker, N. R. Ahern, and A. Y. Wong, *Phys. Rev. Lett.* **20**, 7 (1968).
2. R. J. Briggs, J. D. Daugherty, and R. H. Levy, *Phys. Fluids* **13**, 421 (1970).
3. R. W. Gould, *Phys. Plasmas* **2**, 6 (1994).
4. J. Vanneste, P. J. Morrison, T. Warn, *Phys. Fluids* **10**, 1398 (1998); D. A. Bachman, Ph.D. dissertation, California Institute of Technology (1997).
5. C. F. Driscoll and K. S. Fine, *Phys. Fluids B* **2**, 1359 (1990).
6. T. M. O'Neil and R. W. Gould, *Phys. of Fluids* **11**, 1 (1968).
7. A. J. Peurrung and J. Fajans, *Phys. Fluids B* **5**, 12 (1993).